Modeling carbon nanostructures with the self-consistent charge density-functional tight-binding method: Vibrational spectra and electronic structure of C 28 , C 60 , and C 70

Henryk A. Witek, Stephan Irle, Guishan Zheng, Wibe A. de Jong, and Keiji Morokuma

Citation: The Journal of Chemical Physics **125**, 214706 (2006); doi: 10.1063/1.2370877
View online: http://dx.doi.org/10.1063/1.2370877
View Table of Contents: http://scitation.aip.org/content/aip/journal/jcp/125/21?ver=pdfcov
Published by the AIP Publishing

Articles you may be interested in

Structure and Properties of Magnetic (Co, Fe, Fe 3 C and Ni) Carbon Beads
AIP Conf. Proc. **1311**, 231 (2010); 10.1063/1.3530017

CCSD calculations on C 14 , C 18 , and C 22 carbon clusters
J. Chem. Phys. **128**, 114301 (2008); 10.1063/1.2838200

Predicting the amount of carbon in carbon nanotubes grown by C H 4 rf plasmas
J. Appl. Phys. **99**, 014302 (2006); 10.1063/1.2150599

Analysis of microstructure of magnetic Fe 3 C nanograins embedded in amorphous carbon films
J. Appl. Phys. **94**, 1975 (2003); 10.1063/1.1589590

Magnetic properties of Fe 3 C nanograins embedded in carbon matrix
J. Appl. Phys. **93**, 8462 (2003); 10.1063/1.1555852

This article is copyrighted as indicated in the article. Reuse of AIP content is subject to the terms at: http://scitation.aip.org/termsconditions. Downloaded to IP: 140.113.38.11 On: Wed, 30 Apr 2014 06:23:16

Modeling carbon nanostructures with the self-consistent charge density-functional tight-binding method: Vibrational spectra and electronic structure of C_{28}, C_{60}, and C_{70}

Henryk A. Witek[a),b)]
Institute of Molecular Science, National Chiao Tung University, Hsinchu 300, Taiwan; Department of Applied Chemistry, National Chiao Tung University, Hsinchu 300, Taiwan; and Cherry L. Emerson Center for Scientific Computation, Department of Chemistry, Emory University, Atlanta, Georgia 30322

Stephan Irle[a),c)]
Cherry L. Emerson Center for Scientific Computation, Department of Chemistry, Emory University, Atlanta, Georgia 30322 and Fukui Institute for Fundamental Chemistry, Kyoto University, Kyoto 606-8103, Japan

Guishan Zheng
Cherry L. Emerson Center for Scientific Computation, Department of Chemistry, Emory University, Atlanta, Georgia 30322

Wibe A. de Jong
Environmental Molecular Sciences Laboratory, Pacific Northwest National Laboratory, Richland, Washington 99352

Keiji Morokuma[a),d)]
Cherry L. Emerson Center for Scientific Computation, Department of Chemistry, Emory University, Atlanta, Georgia 30322 and Fukui Institute for Fundamental Chemistry, Kyoto University, Kyoto 606-8103, Japan

(Received 13 July 2006; accepted 27 September 2006; published online 4 December 2006)

The self-consistent charge density-functional tight-binding (SCC-DFTB) method is employed for studying various molecular properties of small fullerenes: C_{28}, C_{60}, and C_{70}. The computed bond distances, vibrational infrared and Raman spectra, vibrational densities of states, and electronic densities of states are compared with experiment (where available) and density-functional theory (DFT) calculations using various basis sets. The presented DFT benchmark calculations using the correlation-consistent polarized valence triple zeta basis set are at present the most extensive calculations on harmonic frequencies of these species. Possible limitations of the SCC-DFTB method for the prediction of molecular vibrational and optical properties are discussed. The presented results suggest that SCC-DFTB is a computationally feasible and reliable method for predicting vibrational and electronic properties of such carbon nanostructures comparable in accuracy with small to medium size basis set DFT calculations at the computational cost of standard semiempirical methods. © *2006 American Institute of Physics*. [DOI: 10.1063/1.2370877]

I. INTRODUCTION

The discovery of fullerene molecules and carbon nanotubes ushered in a new era of nanoscience and nanotechnology.[1] Very unique and intriguing physical properties of these molecules attracted numerous researchers all over the world, although experimental characterization of carbon nanomaterials molecules is very often difficult. Unfortunately, theoretical prediction of properties that could assist in the characterization is not easy due to the large number of atoms, which makes it very difficult to apply rigorous *ab initio* or first principles electronic structure methods. Quantum chemical treatment is very important for π-conjugated carbon networks to describe properly sp^2-carbon based nanomaterials formation and chemistry.[2,3] Conventional single-determinant wave-function-based quantum chemical methods are currently capable to calculate energies and optimized geometries for relatively simple systems containing up to a few hundreds of carbon atoms. For more complex structures, for instance, fullerene assemblies[4] or peapods,[5] it is often necessary to consider explicitly thousands of atoms to obtain a proper description of their structural and chemical properties, rendering conventional quantum chemical methods useless for their modeling. The situation is even more complicated when one wants to compute higher-order molecular properties, for instance, polarizabilities, magnetizabilities, vibrational frequencies, infrared (IR) intensities, and Raman activities; in this case the computational cost usually scales very steeply with the number of particles for rigorous *ab initio* based methods.[6] Even the most advanced parallel implementations of Hartree-Fock (HF) and density-functional theory (DFT) do not currently

[a)]Authors to whom correspondence should be addressed.
[b)]Electronic mail: hwitek@mail.nctu.edu.tw
[c)]Electronic mail: irle@fukui.kyoto-u.ac.jp
[d)]Electronic mail: morokuma@emory.edu

 © 2006 American Institute of Physics

This article is copyrighted as indicated in the article. Reuse of AIP content is subject to the terms at: http://scitation.aip.org/termsconditions. Downloaded to IP: 140.113.38.11 On: Wed, 30 Apr 2014 06:23:16

allow to go beyond a hundred atoms with 1000+ basis functions for the calculation of analytical second derivatives,[7] while the numerical evaluation of the Hessian is impractical and not accurate.

To find a feasible alternative for the costly conventional quantum chemical methods in case of large systems, a considerable part of scientific activity is devoted to develop algorithms that significantly reduce computational time while preserving accuracy as much as possible. The most promising ideas are connected to concepts of localized molecular orbitals,[8] density-fitting techniques,[9] integral approximation,[10] and order *N* methods,[11] but the prediction of second- or higher-order quantities is still not feasible for systems with more than about 100 atoms with such clever mathematical approximations.[12] Another group of methods that receive recently much attention is known under the common name of semiempirical techniques. Born from the necessity that in the early days of quantum chemistry computers were not fast enough to deal with a rigorous formulation of HF and configuration interaction (CI) theory, semiempirical methods utilize a large number of approximations that concern usually both physical and mathematical aspects of the formalism and are generally considered to be less accurate. The self-consistent charge density-functional tight-binding (SCC-DFTB) method of Elstner and coworkers is a very successful method that uses a second-order expansion of the DFT electron density and two-center repulsive energy curves fitted to high-level DFT dissociation curves of model compounds.[13,14] It combines in that sense empirical and mathematical approximations to DFT and is of comparable computational speed as "more conventional" semiempirical methods such as AM1 (Ref. 15) and PM3.[16] It has been applied for calculations of reaction energies and molecular geometries, showing very good agreement to experimental data,[14,17,18] and performs better than AM1 and PM3 methods regarding fullerene isomer geometries and energetics relative to B3LYP/6-31G(*d*) data.[19] DFTB has also been employed in quantum chemical molecular dynamics simulations, which revealed that the dynamic self-assembly of buckminsterfullerene C_{60} follows a "shrinking hot giant" road of fullerene formation.[3,20] Recently, the present authors developed an analytical formulation of second-order derivatives for the SCC-DFTB method that allows for calculating analytical Hessian and harmonic vibrational frequencies.[21–23] The preliminary tests performed for a set of small and medium size molecules show that SCC-DFTB can be used for reproducing experimental fundamental frequencies and IR and Raman spectra in a satisfactory manner. It has been shown that it is possible to remove all large discrepancies between the calculated and experimental vibrational frequencies by refitting the original SCC-DFTB two-body potentials;[24] energies and optimized geometries computed using the reoptimized potentials do not show significant worsening.

The present paper represents a benchmark for the applicability of SCC-DFTB towards prediction of vibrational spectra of fullerene-based carbon nanomaterials for future employment in the assignment of experimental vibrational spectra. We selected three closed-shell fullerenes D_2 C_{28}, I_h C_{60}, and D_{5h} C_{70} as benchmark systems for a comparative study. Molecular structures and IR and Raman vibrational spectra obtained with SCC-DFTB are compared to experimental results (where available), to the C_{60} and C_{70} scaled B3LYP/6-31G(*d*) IR and Raman harmonic vibrational spectra of Schettino *et al.*[25] and Sun and Kertesz,[26] respectively, and to our own unscaled BLYP DFT vibrational spectra, featuring a small 3-21G,[27] a medium 6-31G(*d*),[28] and a large cc-pVTZ (Ref. 29) basis set. In particular, analytical BLYP/cc-pVTZ calculations of vibrational spectra are computationally extremely demanding with 840, 1800, and 2100 basis functions for C_{28}, C_{60}, and C_{70}, respectively, and represent themselves a milestone in the calculation of such highly accurate IR spectra for fullerene systems requiring several weeks of computer wall clock time at the Pacific Northwest Laboratory's EMSL. We selected the BLYP functional to perform a consistent set of benchmark calculations with different basis sets because it is known to predict vibrational frequencies close to experiment even without scaling,[30] in particular, with large pVTZ basis sets.[31] In addition, we performed calculations of the vibrational density of states (VDOS) and the electronic density of states (DOS) for all three molecules at the SCC-DFTB level of theory and compare the results to analogous results determined using BLYP/3-21G, BLYP/cc-pVTZ, and experimental values, where available. For all SCC-DFTB calculations, the new reparametrized repulsive potentials[24] were employed.

II. COMPUTATIONAL DETAILS

All DFTB and SCC-DFTB energy, geometry, and DOS calculations have been performed using a FORTRAN-based program. (Program DYLCAO was written in 1991 by Blaudeck. Further development was due to Porezag and Köhler. The self-consistent formalism was implemented by Elstner.) Harmonic vibrational frequencies, IR intensities, Raman activities, and vibrational densities of states have been obtained using an analytical second derivative module that has been developed in our group.[21] For all DFTB and SCC-DFTB calculations, we have used the new reoptimized repulsive potentials.[24] First principles DFT geometry optimizations were carried out using both B3LYP (Refs. 32 and 33) and BLYP (Ref. 32) density functionals. DFT calculation of vibrational spectra and VDOS was carried out using the BLYP functional only. Results for DOS are only presented for SCC-DFTB and BLYP, as the difference between BLYP and B3LYP density of electronic states is relatively small. Vibrational harmonic frequencies were left unscaled to allow more straightforward comparison between SCC-DFTB and BLYP data. Unless otherwise noted, we employed the 3-21G (Ref. 27) and 6-31G(*d*) (Ref. 28) basis sets for all BLYP calculations using the GAUSSIAN03 suite of programs,[34] while DOS and IR vibrational frequency calculations with the much larger cc-pVTZ basis set were carried out using NWCHEM 4.7 (Ref. 35) at the EMSL Molecular Science Computing Facility. We accepted all default integration grid/convergence threshold parameters of the respective programs for second derivative calculations.

This article is copyrighted as indicated in the article. Reuse of AIP content is subject to the terms at: http://scitation.aip.org/termsconditions. Downloaded to IP: 140.113.38.11 On: Wed, 30 Apr 2014 06:23:16

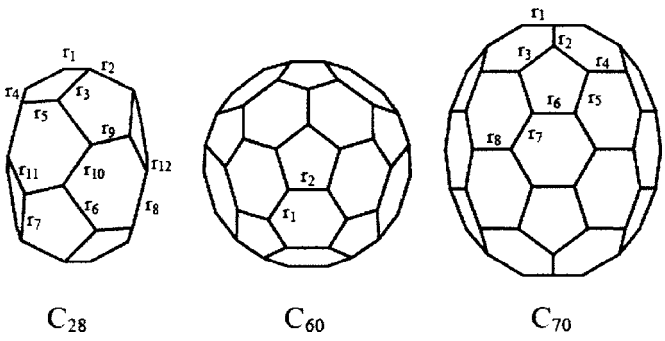

FIG. 1. Symmetry-unique bond distances for D_2 C_{28}, I_h C_{60}, and D_{5h} C_{70}.

III. RESULTS AND DISCUSSION

Our benchmark of the DFTB and SCC-DFTB methods for the prediction of structural, vibrational, and optical properties of fullerene-based carbon nanostructures comprises five related quantities: (1) molecular structures, (2) vibrational frequencies, (3) IR and Raman intensities, (4) vibrational density of states (VDOS), and (5) electronic density of states (DOS). In the following we will discuss each quantity in separate subsections.

A. Optimized geometries

We have optimized the molecular structures of D_2 C_{28}, I_h C_{60}, and D_{5h} C_{70}, which are the lowest-energy isomers except for the case of C_{28}, where a T_d-symmetric structure with quintet electronic ground state is lower in energy. We chose the lowest-energetic singlet electronic state D_2 isomer for C_{28} to avoid complications arising from the somewhat different open-shell treatment in spin-polarized version of DFTB (SCC-sDFTB).[36] We discuss results for both B3LYP and BLYP density functionals in combination with cc-pVTZ and 3-21G basis sets, and we compare the results with SCC-DFTB and DFTB optimized geometries. Relevant optimized molecular structures reported in this work are available in the supplemental material.[59] Symmetry-unique bond distances for C_{28}, C_{60}, and C_{70} structures are given in Fig. 1, and geometrical parameters for the optimized bond distances labeled therein are presented in Table I. We note that the bond distances are generally very similar for all the methods with the largest absolute discrepancy of approximately 0.06 Å. In particular, SCC-DFTB and DFTB show very little deviation, as partial charges of C_{28} and C_{70} are very small (C_{60} has only one symmetry-unique atom with 0 charge, and SCC-DFTB and DFTB results are in this case identical due to symmetry). We reported the similarity of fullerene isomer geometries and energetics already earlier and also elaborated on the comparison between experimental and computed symmetry-unique bond lengths of C_{70}.[19] BLYP has a systematic tendency towards longer bonds by up to 0.022 Å (r_5 of C_{28}) compared to B3LYP, while larger basis sets generally reduce DFT geometries by an average of 0.01 Å difference. The shortening of C=C bonds with the inclusion of polarization functions is a well-known phenomenon; on the other hand,

TABLE I. Optimized geometries of D_2 C_{28}, I_h C_{60}, and D_{5h} C_{70} calculated with various methods. The root mean square deviation σ_{rms} for each method is calculated with respect to the BLYP/cc-pVTZ and B3LYP/cc-pVTZ results. The notation r_i is explained in Fig. 1.

		B3LYP/ cc-pVTZ	BLYP/ cc-pVTZ	B3LYP/ 3-21G	BLYP/ 3-21G	SCC-DFTB	DFTB
C_{28}	r_1	1.461	1.469	1.475	1.483	1.510	1.527
	r_2	1.377	1.400	1.380	1.407	1.407	1.410
	r_3	1.470	1.467	1.495	1.488	1.518	1.519
	r_4	1.498	1.509	1.521	1.530	1.540	1.535
	r_5	1.399	1.419	1.401	1.423	1.424	1.425
	r_6	1.499	1.515	1.505	1.525	1.523	1.516
	r_7	1.445	1.445	1.463	1.462	1.488	1.488
	r_8	1.410	1.414	1.416	1.421	1.441	1.443
	r_9	1.485	1.501	1.490	1.508	1.512	1.516
	r_{10}	1.395	1.403	1.401	1.407	1.421	1.418
	r_{11}	1.395	1.414	1.398	1.419	1.426	1.426
	r_{12}	1.523	1.537	1.545	1.558	1.556	1.556
C_{60}	r_1	1.401	1.401	1.390	1.404	1.411	1.411
	r_2	1.458	1.458	1.460	1.471	1.477	1.477
C_{70}	r_1	1.447	1.457	1.451	1.469	1.476	1.476
	r_2	1.390	1.403	1.409	1.405	1.413	1.413
	r_3	1.443	1.453	1.449	1.466	1.472	1.473
	r_4	1.383	1.396	1.401	1.399	1.403	1.404
	r_5	1.444	1.451	1.449	1.464	1.474	1.474
	r_6	1.430	1.443	1.437	1.452	1.451	1.452
	r_7	1.415	1.426	1.427	1.431	1.438	1.438
	r_8	1.466	1.476	1.461	1.485	1.490	1.488
	σ'_{rms}	0.010	⋯	0.010	0.010	0.019	0.019
	σ_{rms}	⋯	0.010	0.010	0.020	0.029	0.030

This article is copyrighted as indicated in the article. Reuse of AIP content is subject to the terms at: http://scitation.aip.org/termsconditions. Downloaded to IP: 140.113.38.11 On: Wed, 30 Apr 2014 06:23:16

basis set and electron correlation effects are known to partially cancel each other in conjugated systems such as 1,3-butadiene,[37,38] and the "correct" combination is often difficult to evaluate.[38] The only clear exception from the expected basis set dependence of bond lengths is the r_1 bond of C_{60} at the B3LYP level of theory, which is shorter by 0.011 Å than cc-pVTZ in case of the 3-21G basis set and 0.005 Å shorter with respect to 6-31G(d).[39] Solution phase NMR (Ref. 40) and gas phase electron diffraction[41] bond lengths for C_{60} (1.40 and 1.45 Å) are in close agreement with large basis set DFT results (1.401 and 1.458 Å). DFTB bond lengths are longer by 0.01 and 0.02 Å compared to the experimental and large basis set DFT results. A similar comparison of DFTB/SCC-DFTB versus experimental bond lengths in C_{70} yields a more complex picture.[19]

The root mean square deviation σ'_{rms} of SCC-DFTB from BLYP/cc-pVTZ bond lengths for all three fullerenes is 0.019 Å and the σ_{rms} of SCC-DFTB from B3LYP/cc-pVTZ is 0.029 Å, once again indicating that SCC-DFTB agrees better with nonhybrid DFT geometries. We also note that SCC-DFTB and DFTB data tend to reproduce the smaller basis set DFT results; thus DFTB generally predicts the longest partial double bonds in this comparison. The origin for this behavior may be rooted in the fact the atomic parameters of DFTB are determined using the nonhybrid PBE density functional,[18] which itself has a tendency towards longer bond lengths.[42] The overall discrepancy of +0.03 Å compared to B3LYP/cc-pVTZ can, however, be considered relatively harmless given the fact that the still computationally much more expensive BLYP/3-21G exhibits an overall discrepancy of similar magnitude with +0.02 Å. We therefore confirm our previous finding that DFTB and SCC-DFTB can be used as a substitute for more expensive DFT calculations for the structural prediction of fullerene isomer structures.

B. Vibrational frequencies

While we could not find any reported theoretical vibrational data on C_{28}, there are many harmonic vibrational spectra computed at various quantum chemical levels of theory for C_{60} (Refs. 25, 39, and 43) and C_{70} (Refs. 26 and 44) reported in the literature; the references quoted only cite the most recent works which contain more references to other computed IR and Raman spectra of these "popular" fullerenes. Tables II–IV list our theoretical harmonic vibrational frequencies at the BLYP level of theory with cc-pVTZ, 6-31G(d), and 3-21G basis sets and at the SCC-DFTB level of theory. Experimental data for the 14 C_{60} IR and Raman active modes were taken from Ref. 45 and for C_{70} from the compilation by Schettino *et al.*[44] We compare our BLYP results to hybrid DFT B3LYP/6-31G(d) vibrational frequencies computed by Schettino *et al.*[25] for C_{60} and Sun and Kertesz for C_{70}.[26] Both groups reported values using a common scaling factor of 0.98, following an earlier work from 1998 by Stratmann *et al.* on the B3LYP/6-31G(d) calculation of C_{60} IR active modes.[46] For comparison, the recommended uniform scaling factors for B3LYP and BLYP with Sadlej's pVTZ basis set are 0.9726 and 1.0047,[31] respectively. The use of such global scaling factors is problematic, as force constant coupling elements between different C–C and C=C bonds are often highly dependent on the level of electron correlation in a nonpredictable way.[47] Therefore, and to allow a fair comparison between different levels of theory in our benchmark study, all vibrational frequencies were left unscaled, as is good practice in such circumstances.[43] We computed all vibrational frequencies irrespective of their IR or Raman visibility. Since experimental assignments are always subject to change and very difficult for these species due to their many IR and Raman silent modes, we chose the high-level BLYP/cc-pVTZ calculation as reference (ν_i^0) to which we compute root mean square deviations σ_{rsm} as frequency-weighted ($\sigma'_{\mathrm{rms}} = \sqrt{(\Sigma_i w_i(\nu_i - \nu_i^0)^2/\Sigma_i w_i)}, w_i = 1/\nu_i^0$) and unweighted ($\sigma_{\mathrm{rms}}$, $w_i = 1$) quantities. Only when we explicitly discuss deviations from experimental values, the latter become assigned as ν_i^0. The σ_{rms} values are considerably larger than the "average differences" between n experimental and calculated frequencies quoted by Schettino *et al.*,[25,44] which are calculated as $\sqrt{(\Sigma_i w_i(\nu_i - \nu_i^0)^2)}/n$. Weighted and unweighted σ_{rms}'s are typically used to characterize the agreement of calculated vibrational frequency sets with reference data sets and are typically on the order of 10 cm^{-1} in case of excellent agreement, which can usually only be achieved by fitting scaling parameters of individual force constant matrix elements as devised by Pulay *et al.*[48] (see, for instance, Refs. 39 and 49) although global scaling may sometimes succeed as well.[25]

Since the aim of this work is not an elaborate analysis and assignment of the vibrational spectra of C_{28}, C_{60}, and C_{70}, we refer the reader to previous excellent reports discussing the genetic relationship between C_{60} and C_{70} vibrational modes[50] and their symmetry justifications.[44] As it was also pointed out that the number of anharmonic force constants of C_{60} and C_{70} is prohibitively large for an application to achieve a realistic force field comparable to experiment,[51] we are restricting ourselves here to comparisons of harmonic vibrational frequencies with the highest level of theory we could afford, namely, BLYP/cc-pVTZ. In designing our benchmark calculations, it was our hope that the BLYP functional intrinsically provides for a good agreement with experiment, which we found is generally true as will be described in the following paragraphs for each species, C_{28}, C_{60}, and C_{70}.

1. D_2 C_{28}

No experimental vibrational spectra exist on this lowest-energetic closed-shell isomer of C_{28}. We therefore list only harmonic vibrational frequencies at the BLYP/cc-pVTZ, BLYP/6-31G(d), BLYP/3-21G, and SCC-DFTB levels of theory in Table II. All modes are Raman allowed, whereas only B_1, B_2, and B_3 modes are IR active. σ'_{rms} and σ_{rms} values are given with respect to BLYP/cc-pVTZ and are between 13 and 16 cm^{-1} for BLYP data sets obtained with the small and medium basis sets and about 30 cm^{-1} for SCC-DFTB. The difference between weighted σ'_{rms} and unweighted σ_{rms} values is negligible, indicating that no systematic deviation is present in the data sets. The lowest vibrational frequency, which is a B_2 "breathing mode" of the fullerene cage, is predicted to be 284.5 cm^{-1} by BLYP/cc-pVTZ, decreases to

This article is copyrighted as indicated in the article. Reuse of AIP content is subject to the terms at: http://scitation.aip.org/termsconditions. Downloaded to IP: 140.113.38.11 On: Wed, 30 Apr 2014 06:23:16

TABLE II. Harmonic vibrational frequencies (cm^{-1}) of C_{28} (D_2 symmetry) computed using BLYP/cc-pVTZ, BLYP/6-31G(d), BLYP/3-21G, and SCC-DFTB. All modes are Raman active and all B_1, B_2, and B_3 modes are IR active. Root mean square deviations are given with respect to BLYP/cc-pVTZ (ν_i^0) and given as frequency-weighted [$\sigma'_{\mathrm{rms}}=\sqrt{(\Sigma_i w_i(\nu_i-\nu_i^0)^2/\Sigma_i w_i)}, w_i=1/\nu_i^0$] and unweighted ($\sigma_{\mathrm{rms}}, w_i=1$) quantities.

	BLYP			
Symmetry	cc-pVTZ	6-31G(d)	3-21G	SCC-DFTB
A_1	323.0	321.4	324.1	310.9
	416.5	413.0	419.9	411.2
	452.6	449.0	457.4	438.7
	508.7	498.9	508.7	483.4
	591.0	578.9	587.6	547.3
	602.4	592.7	608.3	558.0
	657.5	639.1	652.8	580.5
	673.8	663.3	657.7	621.0
	692.0	674.4	666.9	634.0
	748.2	738.3	758.8	690.2
	869.2	877.2	854.9	846.3
	975.4	977.4	965.7	972.3
	1073.2	1085.2	1049.1	1039.3
	1098.1	1105.7	1085.0	1090.4
	1114.3	1128.7	1094.8	1125.4
	1192.7	1201.3	1195.4	1197.9
	1251.0	1262.0	1225.1	1241.9
	1305.6	1321.7	1297.5	1290.3
	1361.8	1372.7	1360.8	1331.9
	1376.8	1388.0	1377.8	1425.9
	1459.9	1470.1	1459.2	1473.0
B_1	362.2	359.2	373.0	360.6
	463.6	459.0	470.5	458.0
	506.2	497.8	506.8	490.1
	523.3	513.7	524.6	500.4
	642.2	611.5	638.2	539.2
	679.7	647.9	666.9	667.9
	694.8	696.5	694.2	723.2
	717.8	705.2	710.0	731.8
	737.1	719.3	740.3	745.2
	806.6	792.6	825.0	816.3
	951.3	955.8	937.5	957.4
	1073.6	1083.2	1067.0	1061.9
	1113.8	1121.8	1092.5	1112.8
	1173.6	1083.2	1172.3	1162.2
	1220.2	1233.6	1194.0	1220.1
	1328.8	1342.6	1330.5	1297.7
	1351.2	1363.2	1353.0	1407.3
	1390.6	1400.2	1395.8	1411.7
	1429.1	1437.7	1439.3	1444.1
B_2	284.5	277.7	302.0	311.4
	490.0	482.0	480.9	454.8
	513.2	506.8	522.0	513.8
	549.1	534.3	549.9	528.3
	609.2	587.1	606.7	555.4
	639.1	621.2	613.3	586.8
	684.0	657.4	690.1	655.3
	677.5	660.1	664.9	596.8
	740.7	730.1	751.2	750.6
	763.5	763.1	766.8	776.4
	840.7	848.2	830.3	836.8
	959.3	967.3	955.2	957.5
	1027.8	1038.8	1004.2	1026.2
	1144.2	1155.3	1113.7	1107.8
	1156.8	1169.9	1152.9	1174.4

This article is copyrighted as indicated in the article. Reuse of AIP content is subject to the terms at: http://scitation.aip.org/termsconditions. Downloaded to IP: 140.113.38.11 On: Wed, 30 Apr 2014 06:23:16

TABLE II. (*Continued.*)

	BLYP			
Symmetry	cc-pVTZ	6-31G(*d*)	3-21G	SCC-DFTB
	1208.1	1213.1	1191.8	1199.8
	1320.8	1331.2	1325.6	1338.8
	1367.4	1378.5	1364.1	1378.4
	1409.8	1420.8	1410.5	1438.2
B_3	348.0	337.0	366.8	367.2
	437.9	424.8	455.0	429.4
	491.9	479.1	492.8	462.1
	554.8	539.8	556.9	534.9
	588.2	578.9	596.9	562.3
	677.2	644.7	630.2	611.0
	696.0	675.8	678.8	647.2
	697.5	681.8	701.7	693.3
	719.8	712.0	731.3	718.4
	813.6	813.4	809.5	828.3
	863.8	872.1	864.0	888.1
	1001.9	1008.7	993.1	1015.7
	1078.5	1085.5	1064.3	1057.7
	1169.5	1183.7	1144.7	1161.1
	1194.8	1202.3	1197.9	1132.8
	1209.2	1216.9	1175.9	1222.4
	1329.4	1341.1	1329.8	1322.4
	1366.5	1375.3	1375.8	1421.6
	1374.6	1387.1	1368.5	1372.4
σ'_{rms}	⋯	15.2	13.2	32.4
σ_{rms}	⋯	16.4	13.6	31.9

277.7 cm^{-1} at the BLYP/6-31G(*d*) level, and overshoots the cc-pVTZ level with 302.0 cm^{-1} at BLYP/3-21G. The SCC-DFTB value for this mode is 311.4 cm^{-1}, more similar to the small basis set DFT result. This particular behavior of vibrational frequencies with the applied method is, however, not universal, and the tabulated values do not allow to find a systematic trend regarding frequency shifts with the level of theory. We only note one exception, namely, that there exists some systematic blueshift from BLYP/cc-pVTZ to SCC-DFTB for the very highest frequencies, such as B3LYP/cc-pVTZ A_1 1376.8 and 1459.9 cm^{-1}, B_1 1351.2–1429.1 cm^{-1}, B_2 1409.8 cm^{-1}, and B_3 1366.5 and 1374.6 cm^{-1}, with shifts to higher frequencies as large as 50 cm^{-1}.

2. I_h C_{60}

Since the experimental assignment of silent modes other than Raman active A_g and H_g and IR active T_{1u} modes is very difficult,[39] we include only the experimentally visible modes in our benchmark comparison. Here, we also list the scaled and unscaled B3LYP/6-31G(*d*) values reported by Schettino *et al.*[25] in Table III. σ'_{rms} and σ_{rms} for BLYP/cc-pVTZ with respect to experimental values are 22.8 and 27.2 cm^{-1}, respectively (not shown in table), and indicate some systematic underestimation of high frequency modes at the quantum chemical level. The same can be said about the unscaled B3LYP/6-31G(*d*) calculations, where the weighted σ'_{rms} is 19.9 cm^{-1}, whereas the unweighted σ_{rms} is 24.8 cm^{-1} (also not listed). However, the trend for the high vibrational frequencies regarding BLYP and hybrid B3LYP is opposite; the Hartree-Fock contribution in B3LYP causes blueshifting, whereas BLYP tends to predict too small frequencies. Remarkably, when scaling of B3LYP frequencies by 0.98 is applied, the values of σ'_{rms} and σ_{rms} with respect to experimental frequencies drop to 9.4 and 8.5 cm^{-1}. The σ'_{rms} and σ_{rms} for unscaled B3LYP/6-31G(*d*) with respect to BLYP/cc-pVTZ are 34.3 and 44.8 cm^{-1}, respectively, again reflecting a systematic trend in B3LYP data towards higher vibrational frequencies and generally indicating the wide uncertainty of different high-level DFT methods regarding the prediction of even harmonic vibrational frequencies. Compared to B3LYP/6-31G(*d*), SCC-DFTB performs very well in the comparison with BLYP/cc-pVTZ, with σ'_{rms} and σ_{rms} values of 32.2 and 34.4 cm^{-1}, respectively. Since DFTB does not directly contain a contribution from Hartree-Fock exchange, no systematic trend is visible in its deviations from the BLYP data. It even outperforms BLYP/3-21G, which has corresponding deviations of 39.0 and 39.3 cm^{-1} for scaled and unscaled deviations, respectively. Regarding the lowest vibrational frequencies, we note that the fivefold degenerate H_g breathing mode at BLYP/cc-pVTZ 260.2 cm^{-1} is lower compared to C_{28} by 24.3 cm^{-1}, reflecting the larger cage diameter. Its corresponding values at the BLYP/6-31G(*d*), BLYP/3-21G, and SCC-DFTB levels of theory are very similar to 258.4, 259.6, and 254.6 cm^{-1}, respectively. Here, we cannot observe a systematic trend of SCC-DFTB towards blueshifting high vibrational frequen-

This article is copyrighted as indicated in the article. Reuse of AIP content is subject to the terms at: http://scitation.aip.org/termsconditions. Downloaded to IP: 140.113.38.11 On: Wed, 30 Apr 2014 06:23:16

TABLE III. Harmonic vibrational frequencies (cm^{-1}) of C_{60} (I_h symmetry) computed using BLYP/cc-pVTZ, BLYP/6-31G(d), BLYP/3-21G, and SCC-DFTB. Experimental data are taken from Ref. 45. B3LYP/6-31G(d) data are given for comparison. The A_g and H_g modes are Raman active and the T_{1u} modes are IR active. Root mean square deviations are given with respect to BLYP/cc-pVTZ (ν_i^0) and given as frequency-weighted [$\sigma'_{\mathrm{rms}}=\sqrt{(\Sigma_i w_i(\nu_i-\nu_i^0)^2/\Sigma_i w_i)}, w_i=1/\nu_i^0$] and unweighted ($\sigma_{\mathrm{rms}}, w_i=1$) quantities.

		BLYP					
Symmetry	Expt.	cc-pVTZ	6-31G(d)	3-21G	SCC-DFTB	B3LYP[a] 6-31G(d)	B3LYP[b] 6-31G(d)
A_g	496	481.5	479.3	473.7	490.2	487	497
	1470	1431.6	1445.4	1437.5	1384.8	1474	1504
H_g	273	260.2	258.4	259.6	254.6	261	266
	437	429.0	424.1	408.5	412.5	429	438
	710	711.4	691.9	643.2	664.1	705	719
	774	760.0	760.3	751.2	759.7	772	788
	1099	1083.2	1085.9	1069.1	1076.6	1104	1127
	1250	1206.6	1221.4	1174.1	1171.3	1251	1277
	1428	1380.4	1396.4	1372.3	1345.4	1426	1455
	1575	1533.2	1543.9	1533.3	1556.9	1585	1617
T_{1u}	527	531.2	517.6	481.1	485.6	528	539
	557	568.8	568.5	559.7	576.7	577	589
	1183	1160.7	1168.0	1128.9	1137.7	1189	1213
	1428	1389.6	1405.4	1393.1	1347.7	1431	1460
T_{1g}		554.6	548.8	512.9	528.9	562	573
		825.5	811.9	830.7	822.7	823	840
		1249.1	1251.8	1225.8	1233.6	1276	1302
T_{2g}		567.3	549.0	562.5	549.5	555	566
		767.9	716.1	623.8	671.8	724	739
		791.3	780.7	809.0	801.0	789	805
		1295.1	1307.7	1266.4	1273.2	1344	1371
G_g		479.3	473.8	461.2	472.8	480	490
		565.3	561.0	576.7	563.0	565	577
		747.5	723.6	653.4	679.3	741	756
		1049.8	1060.4	1025.9	984.4	1072	1094
		1282.2	1286.8	1271.4	1270.2	1307	1334
		1459.1	1470.8	1453.0	1465.9	1507	1538
A_u		955.2	932.8	973.0	959.4	946	965
T_{2u}		338.2	335.3	332.8	333.0	327	334
		715.8	694.9	642.6	654.0	709	723
		945.8	949.0	933.6	911.3	958	978
		1149.6	1161.4	1122.0	1088.3	1177	1201
		1492.6	1501.7	1499.2	1512.6	1536	1567
G_u		349.5	347.8	340.5	340.1	351	358
		760.7	727.7	636.5	679.9	738	753
		781.8	742.7	766.1	760.4	751	766
		945.0	946.8	933.8	930.1	962	982
		1266.7	1279.3	1245.6	1240.4	1307	1334
		1384.4	1400.3	1367.0	1355.7	1434	1463
H_u		398.9	396.3	402.8	390.6	400	408
		531.6	522.5	506.0	523.6	531	542
		667.0	658.2	639.9	650.4	665	679
		740.2	712.1	689.3	694.0	729	744
		1186.8	1193.7	1163.0	1172.1	1219	1244
		1307.6	1313.7	1283.6	1284.9	1343	1370
		1521.9	1533.4	1518.5	1543.9	1576	1608
σ'_{rms}		⋯	15.0	39.0	32.2	21.5	34.3
σ_{rms}		⋯	15.8	39.3	34.4	27.5	44.8

[a]Scaled values from Ref. 25.
[b]Unscaled values from same reference (multiplied by factor of 1/0.98).

cies; the picture is rather nonuniform. We note, however, that, in particular, in the SCC-DFTB and BLYP/3-21G regions between 600 and 700 cm^{-1}, the basis set effect on the values of these particular frequencies is very significant; in going from 3-21G to cc-pVTZ basis sets, the BLYP vibrational frequencies increase by more than 100 wave numbers with SCC-DFTB being higher than BLYP/3-21G but lower than BLYP/6-31G(d). The nature of these vibrations, invis-

This article is copyrighted as indicated in the article. Reuse of AIP content is subject to the terms at: http://scitation.aip.org/termsconditions. Downloaded to IP: 140.113.38.11 On: Wed, 30 Apr 2014 06:23:16

TABLE IV. Harmonic vibrational frequencies in (cm^{-1}) of C_{70} (D_{5h} symmetry) computed using BLYP/cc-pVTZ, BLYP/6-31G(d), BLYP/3-21G, and SCC-DFTB. Experimental data are taken from the compilation in Ref. 44. B3LYP/6-31G(d) data are given for comparison. The A_1', E_2', and E_1'' modes are Raman active and the E_1' and A_2'' modes are IR active. Root mean square deviations are given with respect to BLYP/cc-pVTZ (ν_i^0) and given as frequency-weighted [$\sigma'_{\mathrm{rms}}=\sqrt{(\Sigma_i w_i(\nu_i-\nu_i^0)^2/\Sigma_i w_i)}$, $w_i=1/\nu_i^0$] and unweighted (σ_{rms}, $w_i=1$) quantities.

		BLYP								BLYP					
Symmetry	Expt.	cc-pVTZ	6-31G(d)	3-21G	SCC-DFTB	B3LYP[a] 6-31G(d)	B3LYP[b] 6-31G(d)	Symmetry	Expt.	cc-pVTZ	6-31G(d)	3-21G	SCC-DFTB	B3LYP[a] 6-31G(d)	B3LYP[b] 6-31G(d)
A_1'	260	254.0	249.8	253.7	247.2	253	258	E_1'	328	324.4	320.1	320.5	316.7	326	332
	396	394.1	386.6	383.1	382.6	393	401		361	358.0	353.5	359.8	351.3	358	366
	455	444.8	441.6	437.0	457.8	448	457		418	417.7	406.7	398.5	401.5	415	423
	568	556.1	550.8	520.8	524.4	565	576		509	507.5	497.7	486.2	493.1	507	518
	697	691.2	689.7	684.2	700.3	701	716		534	528.4	524.1	517.8	535.7	533	544
	701	715.0	692.5	645.6	657.1	709	723		578	557.1	558.2	532.4	546.3	573	585
	1060	1047.2	1044.8	1039.8	1045.0	1061	1083		642	580.4	629.8	598.0	610.8	640	653
	1182	1146.7	1157.3	1124.9	1132.0	1185	1209		674	644.0	653.5	635.1	651.8	666	679
	1222	1199.9	1208.8	1170.1	1163.0	1229	1254		728	676.3	711.1	645.3	686.0	729	744
	1459	1398.3	1411.3	1377.6	1373.0	1450	1479		795	803.8	737.6	674.9	696.6	751	767
	1468	1428.1	1438.9	1426.8	1440.0	1472	1502		835	828.8	815.3	836.7	834.0	828	845
	1576	1523.9	1533.5	1527.6	1543.0	1574	1606		904	889.5	889.4	886.1	894.2	905	923
E_2'	225	222.2	216.7	218.6	214.2	220	224		1087	1063.0	1066.2	1050.8	1066.0	1087	1109
	303	301.4	294.3	292.7	292.0	299	305		1176	1153.3	1156.3	1136.8	1133.0	1177	1201
	430	426.9	418.7	415.1	417.8	426	435		1251	1218.3	1226.6	1188.9	1200.0	1255	1280
	505	503.8	492.4	485.7	495.4	502	513		1291	1259.2	1262.2	1238.7	1248.0	1290	1317
	535	518.1	526.6	537.7	527.2	534	544		1321	1289.1	1294.3	1275.9	1281.0	1318	1345
	668	666.5	656.1	627.0	640.6	665	679		1414	1374.2	1382.0	1351.7	1382.0	1415	1444
	688	699.3	673.6	643.5	651.7	689	703		1430	1390.9	1403.6	1380.3	1356.0	1431	1460
	721	730.8	708.3	686.9	680.2	722	737		1489	1443.1	1450.8	1427.1	1480.0	1489	1519
	738	766.1	720.9	635.9	688.9	735	750		1563	1516.0	1526.8	1514.1	1531.0	1569	1601
	743	772.4	727.0	721.6	696.7	741	756	A_2'	490	489.6	476.1	466.6	478.2	485	495
	760	773.6	733.5	784.6	739.5	750	766		543	546.0	538.3	575.8	542.6	546	557
	768	791.8	756.9	651.7	783.9	767	782		621	642.1	614.7	550.0	595.2	629	642
	948	928.7	928.5	1025.6	941.3	945	964		⋯	754.8	725.7	623.4	688.6	732	747
	1055	1042.0	1045.5	926.2	1004.0	1059	1081		750	785.9	733.7	751.5	747.5	745	760
	1196	1160.2	1162.5	1145.8	1161.0	1187	1211		938	943.4	922.0	961.5	950.7	936	955
	1258	1225.4	1232.9	1203.4	1200.0	1257	1283		1215	1187.2	1188.6	1168.5	1199.0	1215	1240
	1332	1287.3	1298.3	1267.2	1272.0	1329	1356		1342	1304.7	1311.3	1290.4	1296.0	1338	1366
	1349	1313.6	1319.2	1313.0	1292.0	1349	1377		1442	1412.5	1417.3	1395.0	1433.0	1450	1480
	1374	1330.1	1341.4	1288.4	1327.0	1373	1401	A_1''	337	336.6	332.2	338.1	327.9	336	343
	1500	1459.1	1465.8	1450.3	1466.0	1501	1532		527	535.3	515.6	490.9	500.7	529	540
	1520	1475.8	1485.6	1462.7	1512.0	1523	1554		609	613.5	604.5	622.4	611.1	612	624
	1580	1519.9	1529.4	1514.4	1542.0	1573	1605		⋯	743.7	717.5	656.3	694.1	734	749
E_1''	250	246.9	242.0	246.6	240.2	245	250		785	799.0	768.0	790.4	783.6	779	795
	410	409.4	401.6	395.4	394.4	408	417		892	898.0	879.6	910.7	900.7	892	910
	480	480.2	468.1	451.0	456.2	479	488		1241	1218.6	1219.2	1196.8	1202.0	1240	1266
	520	517.2	508.0	500.9	499.8	515	525		⋯	1309.2	1312.8	1279.3	1290.0	1347	1375
	548	533.5	535.7	534.9	533.2	546	557		1550	1508.4	1517.1	1492.0	1534.0	1558	1590
	675	676.3	665.2	643.2	660.9	675	688	E_2''	309	306.1	300.2	303.2	299.9	304	311
	712	718.6	697.6	650.8	687.5	714	728		382	382.3	376.7	372.8	368.3	383	390
	733	745.0	720.6	691.9	691.7	735	750		412	407.1	400.3	405.0	396.0	407	415
	741	770.1	724.8	721.6	733.0	740	755		522	551.2	504.9	496.0	508.4	515	525
	800	797.4	783.9	807.1	804.7	794	811		557	635.9	549.1	566.6	553.8	555	567
	1050	1038.3	1039.2	1023.8	1013.0	1054	1076		⋯	709.6	626.6	633.0	629.1	633	646
	1172	1145.7	1149.3	1122.0	1132.0	1169	1193		690	726.7	684.9	634.9	663.1	701	715
	1227	1189.6	1198.1	1161.3	1195.0	1226	1251		709	731.5	700.0	646.7	671.9	717	732
	1227	1261.1	1267.9	1239.9	1252.0	1296	1323		726	746.1	719.6	653.7	679.1	728	742
	1311	1286.8	1291.3	1270.3	1271.0	1313	1340		790	786.3	771.5	800.0	796.7	781	797
	1367	1333.9	1342.6	1309.4	1316.0	1366	1394		922	907.9	907.0	899.3	902.1	920	939
	1445	1389.1	1403.0	1379.4	1354.0	1432	1461		1070	1057.1	1056.8	1047.3	1060.0	1075	1096

This article is copyrighted as indicated in the article. Reuse of AIP content is subject to the terms at: http://scitation.aip.org/termsconditions. Downloaded to IP: 140.113.38.11 On: Wed, 30 Apr 2014 06:23:16

TABLE IV. (*Continued.*)

		BLYP								BLYP					
Symmetry	Expt.	cc-pVTZ	6-31G(*d*)	3-21G	SCC-DFTB	B3LYP[a] 6-31G(*d*)	B3LYP[b] 6-31G(*d*)	Symmetry	Expt.	cc-pVTZ	6-31G(*d*)	3-21G	SCC-DFTB	B3LYP[a] 6-31G(*d*)	B3LYP[b] 6-31G(*d*)
	1511	1469.2	1478.3	1454.9	1485.0	1516	1546		1152	1132.4	1140.7	1106.1	1073.0	1156	1179
	1545	1521.7	1531.9	1520.5	1547.0	1574	1606		1261	1219.6	1229.0	1189.2	1200.0	1258	1283
A_2''	320	320.5	314.4	318.2	316.4	318	324		1316	1276.4	1286.6	1280.9	1265.0	1316	1343
	458	461.9	450.3	434.1	438.1	459	468		1338	1295.8	1299.1	1251.6	1299.0	1327	1354
	564	507.6	554.9	549.4	568.1	564	575		1400	1355.7	1368.9	1341.4	1354.0	1399	1427
	707	709.7	687.6	642.9	661.9	704	718		1455	1409.9	1422.3	1389.2	1393.0	1455	1484
	901	890.9	888.3	877.8	870.2	896	914		1528	1474.3	1482.6	1471.5	1498.0	1517	1547
	1133	1115.2	1118.7	1096.7	1123.0	1143	1166		1565	1520.7	1529.5	1515.7	1546.0	1573	1605
	1203	1179.3	1190.7	1150.2	1164.0	1206	1230	σ'_{rms}	24.9	⋯	21.7	40.3	29.5	25.5	36.5
	1320	1289.7	1304.7	1271.3	1272.0	1321	1348	σ_{rms}	29.3	⋯	21.4	41.6	30.4	30.2	46.2
	1460	1423.3	1434.1	1422.6	1383.0	1462	1492								
	1557	1519.9	1529.2	1525.7	1538.0	1568	1600								

[a]Scaled values from Ref. 26.
[b]Unscaled values from same reference (multiplied by factor of 1/0.98).

ible in IR and Raman, is described as a deformation of the pentagon rings corresponding to out-of-plane motion of its C_2 units. In particular, we note that even for transition from BLYP/6-31G(*d*) to BLYP/cc-pVTZ, corresponding changes can be as large as 50 wave numbers [for instance, T_{2g} BLYP/cc-pVTZ with 767.9 cm^{-1}, up from 716.1 cm^{-1} at BLYP/6-31G(*d*) and 623.8 cm^{-1} at BLYP/3-21G]. While we cannot explain at this moment the origin of this strong basis set dependence for these particular pentagon modes, we note that SCC-DFTB performs reasonably well as a minimum basis set method.

3. D_{5h} C_{70}

In this case, we compare our results (Table IV) with experimental vibrational frequencies available for all irreducible representations from the compilation in Ref. 44 and with the scaled and unscaled B3LYP/6-31G(*d*) values reported by Sun and Kertesz.[26] The values of σ'_{rms} and σ_{rms} for BLYP/cc-pVTZ with respect to experimental values are 24.9 and 29.3 cm^{-1}, respectively, and again indicate some systematic underestimation of high frequency modes at the quantum chemical level, as was the case before with C_{60}. A similar behavior is also seen for the unscaled B3LYP/6-31G(*d*) calculations, where the weighted σ'_{rms} with respect to experimental frequencies is 18.2 cm^{-1}, whereas the unweighted σ_{rms} is 23.0 cm^{-1} (not listed). Again, B3LYP tends to overestimate vibrational frequencies, while BLYP does not show a clear trend. It is indeed astonishing how similar these values are compared to C_{60}, especially considering the fact that now all 122 symmetry-unique vibrational frequencies are taken into account. When scaling of B3LYP frequencies by 0.98 is applied, the values of σ'_{rms} and σ_{rms} with respect to experimental frequencies drop to 7.8 and 9.2 cm^{-1}, as was shown by Sun and Kertesz.[26] The values of σ'_{rms} and σ_{rms} for unscaled B3LYP/6-31G(*d*) with respect to BLYP/cc-pVTZ are 36.5 and 46.2 cm^{-1}, respectively, again indicating the wide uncertainty of different high-level DFT methods regarding the prediction of harmonic vibrational frequencies. Compared to B3LYP/6-31G(*d*), SCC-DFTB performs similarly very well as in the case of C_{60} in the comparison with BLYP/cc-pVTZ, with σ'_{rms} and σ_{rms} values of 29.5 and 30.4 cm^{-1}, respectively. It again outperforms BLYP/3-21G, which has corresponding deviations of 40.3 and 41.6 cm^{-1} for scaled and unscaled deviations, respectively. Again, it is striking how similar the level-specific σ'_{rms} and σ_{rms} values for C_{60} and C_{70} species are, indicating the common nature between the two sets of vibrational modes.[44,50] Regarding the lowest vibrational frequencies, we note that the lowest E'_2 vibrational mode related to the fivefold degenerate C_{60} breathing modes at BLYP/cc-pVTZ 222.2 cm^{-1} is even lower compared to C_{60} by 38.0 cm^{-1}, reflecting the increase in cage diameter. Its corresponding values at the BLYP/6-31G(*d*), BLYP/3-21G, and SCC-DFTB levels of theory are again very similar with 216.7, 218.6, and 214.2 cm^{-1}. As was the case in C_{60}, we cannot observe a systematic trend of SCC-DFTB towards blueshifting high vibrational frequencies; the picture is rather nonuniform. We also note again the systematic blueshift of modes around 600 and 700 cm^{-1} at SCC-DFTB and BLYP/3-21G levels of theory; some vibrational frequencies are becoming higher with the increase in basis set, but to a somewhat lesser degree than in the case of C_{60}. These modes are also related to pentagon out-of-plane deformations. Here, we have more experimental data to compare with, and somewhat surprisingly we find that the corresponding experimental vibrational frequencies are almost always *lower* than the BLYP/cc-pVTZ data, indicating that the theory is overshooting in these modes with an increase in the size of basis set. This is "good news" for the SCC-DFTB method, which happens to predict in this case vibrational frequencies in similar agreement with experiment than BLYP/cc-pVTZ although systematically redshifted.

This article is copyrighted as indicated in the article. Reuse of AIP content is subject to the terms at: http://scitation.aip.org/termsconditions. Downloaded to IP: 140.113.38.11 On: Wed, 30 Apr 2014 06:23:16

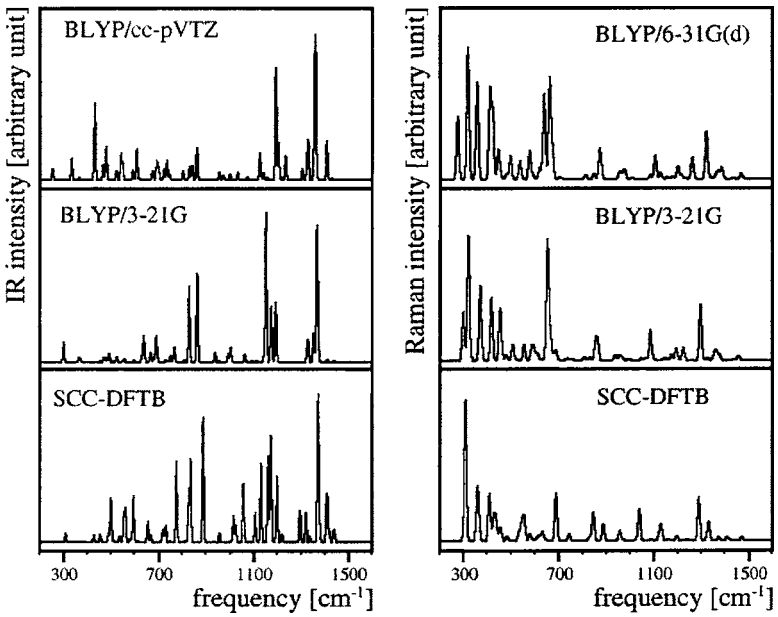

FIG. 2. Vibrational IR and Raman spectra of D_2 C_{28}.

C. IR and Raman spectra

Experimental vibrational Fourier transform infrared (FTIR) spectra of C_{60} and C_{70} have been taken from Bethune *et al.*[45] (Figs. 3 and 4) and analogous FT-Raman spectra from Lynch *et al.*[52] (also Figs. 3 and 4). The FTIR spectra were recorded with sample films on KBr and the Raman spectra, with crystalline samples. For C_{28}, for which no experimental data are available, we compare the calculated spectra with the BLYP/cc-pVTZ IR spectrum and the BLYP/6-31G(*d*) Raman spectrum. The combined experimental (where available) and theoretical vibrational IR and Raman spectra for C_{28}, C_{60}, and C_{70} are presented in Figs. 2–4, respectively, with BLYP/cc-pVTZ IR spectra as highest level of theory in case of IR spectra and BLYP/6-31G(*d*) in case of computed Raman spectra. The Raman intensities have been obtained from calculated Raman activities using the procedure described in Ref. 22. The necessary parameters (ν_{laser}=9398.5 cm^{-1} and T=25 °C) are taken from experiment.

When comparisons between experimental and theoretical Raman spectra are discussed, one should keep in mind that experimental Raman intensities depend very strongly on the wavelength of the exciting laser, state of the sample, and the temperature of the experiment. It is very difficult to compare Raman spectra obtained in different experimental conditions. To enable comparison of various measurements, another quantity is rather employed called Raman activity. The dependence of Raman activities on the laser wavelength and temperature is much smaller. Raman activities can be computed in an easy manner from invariants of the polarizability derivative tensor and are the quantities computed by popular quantum chemistry packages, for example, in GAUSSIAN. It is very important to stress here that the Raman activities determined from quantum chemical calculations cannot be directly compared with observed Raman intensities, since the relationship between these two sets of quantities is very nonlinear. Unfortunately, this mistake is very common while reporting Raman spectra.

Notwithstanding this principal obstacle, we note that the overall quality of the SCC-DFTB IR and Raman spectra is surprisingly good, even when compared to the experimental C_{60} and C_{70} spectra, although Raman intensities, in particular, in the case of C_{60} are somewhat problematic for the reasons mentioned above, specifically, the peaks at 500 and 1500 cm^{-1}, where all quantum chemical methods predict largely different Raman intensities. The IR and Raman spectra for C_{60} and C_{70} calculated with SCC-DFTB and with BLYP/3-21G are almost identical with small deviations concerning the intensity of some peaks. They match also well the experimental findings (the experimental spectra were recorded not in gas-phase but for solid-state fullerences, which may affect substantially the observed intensities). The largest discrepancies regarding the SCC-DFTB relative intensities compared with those predicted from BLYP can be observed for C_{28}. In this case, all three calculated spectra corresponding to different quantum chemical methods, both for IR and Raman, show some similarities; however, it would be difficult to conclude that they correspond to the same molecule. This is particularly true for the IR spectrum in the 800 cm^{-1} region, where SCC-DFTB and BLYP/3-21G predict the existence of two large-intensity peaks, whereas BLYP/cc-pVTZ predicts rather low intensity peaks instead. The computed spectra suggest that the size of the basis set can be crucial for calculating IR and Raman spectra for C_{28}. The corresponding properties of C_{60} and C_{70} are much less dependent on the size of basis set. The origin of the special behavior of C_{28} regarding IR and Raman intensities can be seen in its much smaller highest occupied molecular orbital–lowest unoccupied molecular orbital (HOMO-LUMO) gap than for the other two fullerene molecules; its values determined with DFT/BLYP/cc-pVTZ are 0.52 eV for C_{28}, 1.66 eV for C_{60}, and 1.69 eV for C_{70}. Smaller gap usually denotes larger open-shell character of a given molecule and increases the contribution of low-lying virtual molecular levels on the properties of the system.

This article is copyrighted as indicated in the article. Reuse of AIP content is subject to the terms at: http://scitation.aip.org/termsconditions. Downloaded to IP: 140.113.38.11 On: Wed, 30 Apr 2014 06:23:16

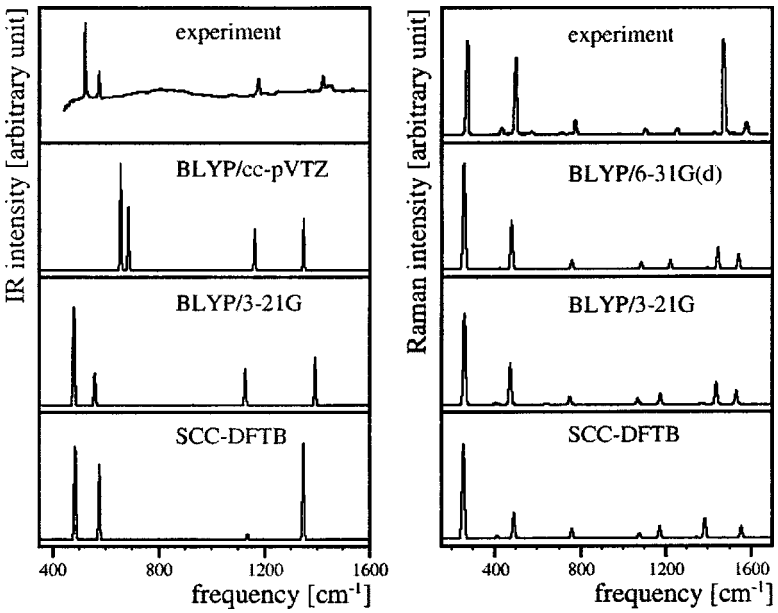

FIG. 3. Experimental and theoretical vibrational IR and Raman spectra of I_h C_{60}.

D. Vibrational density of states (VDOS)

The VDOS is normally calculated for solid systems by performing Fourier analysis of the velocity-velocity autocorrelation function[53] and usually yields information about vibrational properties of such extended systems with respect to energy and spatial localization of particular vibrational modes ("phonons"). In order to make the results of our vibrational frequency benchmark analysis applicable to nanoscale systems, we simulate a VDOS of all modes irrespective of their optical activities obtained as a superposition of Gaussian peaks (half-width=35.3 cm^{-1}) corresponding to discrete vibrational frequencies discussed in Sec. III B. The experimental and theoretical VDOSs of C_{28}, C_{60}, and C_{70} are presented in Fig. 5 and are used to show the performance of the SCC-DFTB method for all vibrational states that are crucial for determining various thermodynamic properties, for instance, entropy. We visually compare the calculated SCC-DFTB VDOS with experimental data and with BLYP/cc-pVTZ and BLYP/3-21G results except for C_{28}, where no experimental data are available.

For C_{60} and C_{70}, the correspondence of the SCC-DFTB and BLYP/3-21G vibrational densities of states is surprisingly good; this is so even though the σ_{rms} between these data sets (not discussed above) is rather large with 29.9 cm^{-1} (C_{28}), 19.8 cm^{-1} (C_{60}), and 26.4 cm^{-1} (C_{70}). We find it remarkable that data sets with relatively large σ_{rms} can produce similarly looking VDOS, an indication that the quality of predicted vibrational frequencies cannot be reduced to a single number such as the average deviation from a reference data set. In particular, a large peak around 650 cm^{-1} can be seen for all four VDOSs of C_{60} and C_{70}, which correspond mainly to highly degenerate C_2 out-of-plane rotations in pentagons, all of which being dark or having low IR or Raman intensities. This large band experiences the largest blueshift

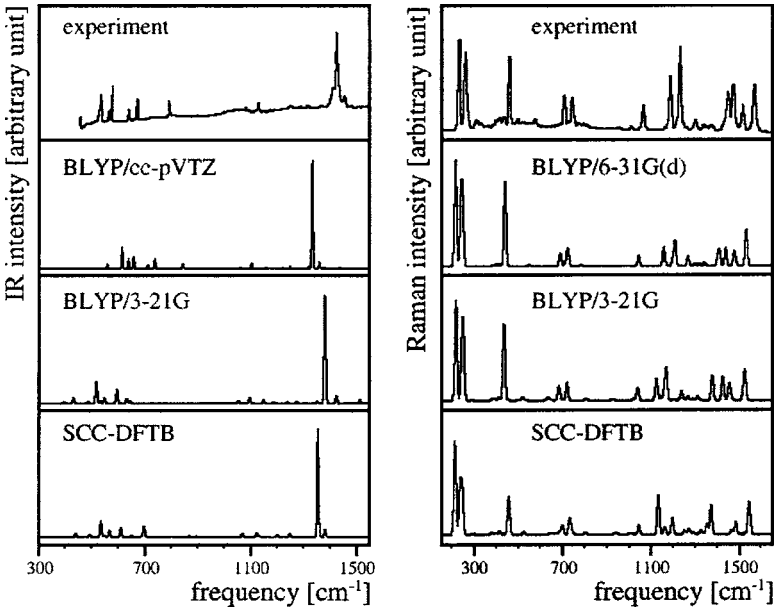

FIG. 4. Experimental and theoretical vibrational IR and Raman spectra of D_{5h} C_{70}.

This article is copyrighted as indicated in the article. Reuse of AIP content is subject to the terms at: http://scitation.aip.org/termsconditions. Downloaded to IP: 140.113.38.11 On: Wed, 30 Apr 2014 06:23:16

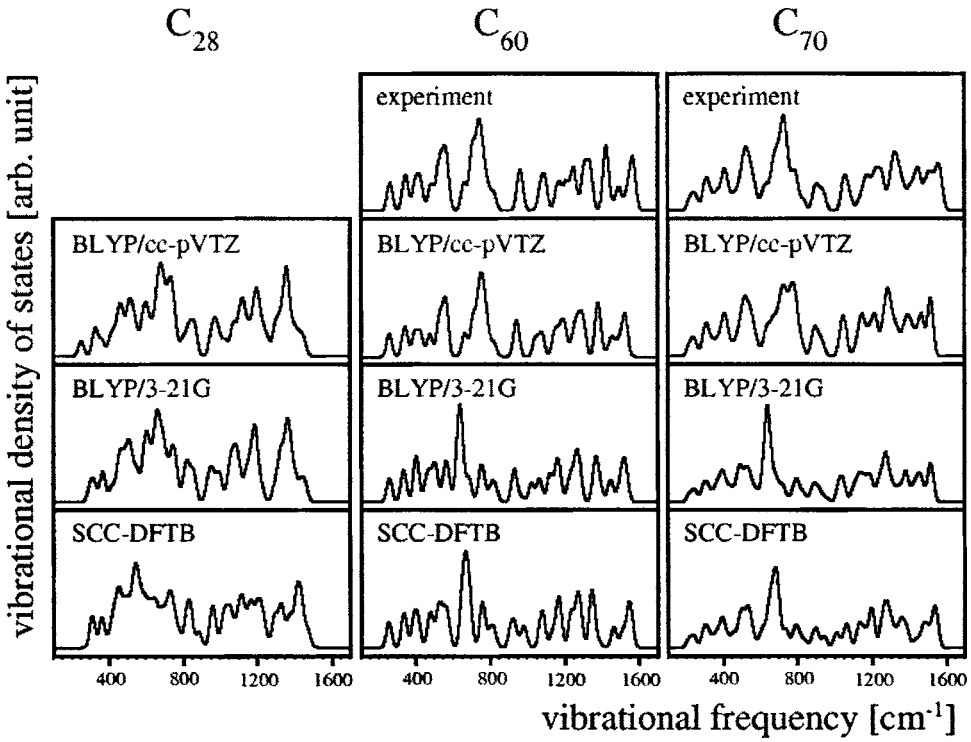

FIG. 5. Calculated and experimental vibrational density of states (VDOS) for D_2 C_{28}, I_h C_{60}, and D_{5h} C_{70}.

with increasing basis set size, as discussed in Sec. III B, which is why its peak can be found between 700 and 800 cm^{-1} for both VDOSs from experiment and BLYP/cc-pVTZ. Concerning the features below 650 cm^{-1}, all four VDOSs of each C_{60} and C_{70} species share the same feature of four peaks increasing in intensity with increasing frequencies. Above 800 cm^{-1}, the features are not very clear and it is hard to establish a plausible correspondence between VDOS peaks. Overall, the correspondence of the VDOS predicted by SCC-DFTB to that of large basis set BLYP/cc-pVTZ and experimental VDOS is rather mediocre, with the exception of C_{28}, where the theoretical curves show similar overall shapes. In the cases where experimental data are available (C_{60} and C_{70}), the experimental VDOS is not surprisingly very similar in shape compared to the corresponding BLYP/cc-pVTZ (most accurate) theoretical data set. In conclusion, we find that SCC-DFTB mimics the VDOS of small basis set DFT calculations and correctly predicts its general features

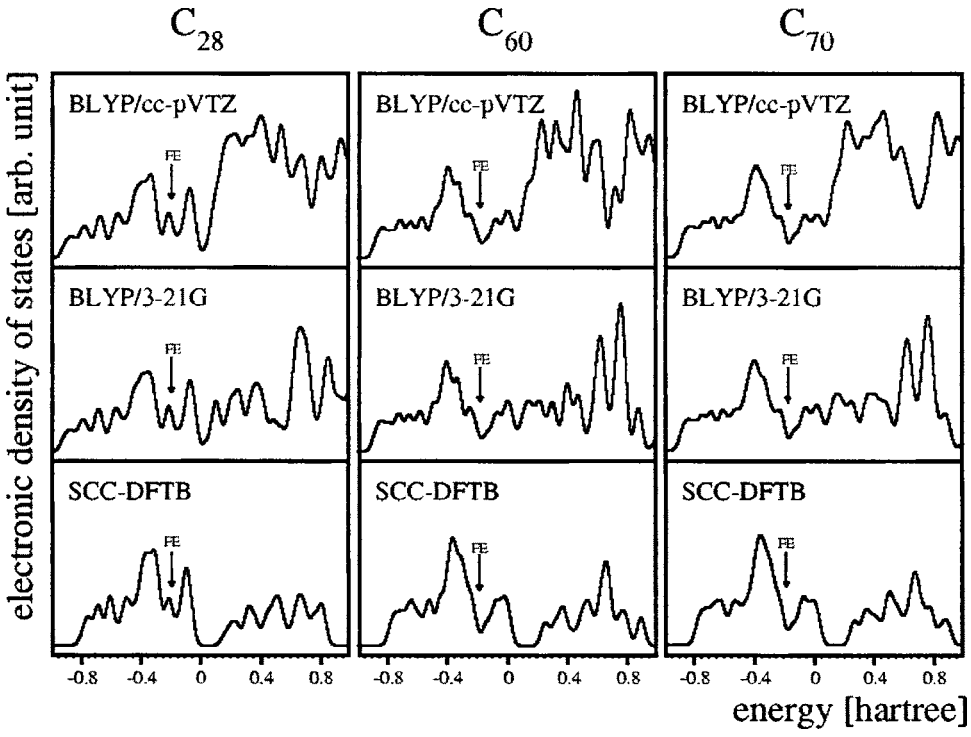

FIG. 6. Calculated electronic densities of states (DOSs) for D_2 C_{28}, I_h C_{60}, and D_{5h} C_{70}.

This article is copyrighted as indicated in the article. Reuse of AIP content is subject to the terms at: http://scitation.aip.org/termsconditions. Downloaded to IP: 140.113.38.11 On: Wed, 30 Apr 2014 06:23:16

TABLE V. Fermi level energies (eV) for C_{28}, C_{60}, and C_{70}. See text for the definition of the Fermi levels.

	C_{28}	C_{60}	C_{70}
BLYP/cc-pVTZ	−5.11	−4.72	−4.69
BLYP/3-21G	−5.16	−4.71	−4.66
SCC-DFTB	−5.17	−4.98	−4.97

even when compared to experimental or larger basis set DFT calculations; however, care needs to be taken concerning position and exact shape of peaks.

E. Electronic density of state (DOS)

Although the eigenstates of the fullerene electronic Hamiltonian are typically discussed in terms of molecular orbitals (MOs) with degeneracy relationships dictated by the high molecular symmetries,[54] the electronic structures of fullerene-containing nanoscale systems such as peapods are typically discussed in terms of electronic density of states (DOS),[55] here computed with 0.059 a.u. Gaussian half-width. It is for this reason that we present here the DOS of C_{28}, C_{60}, and C_{70} calculated at the BLYP/cc-pVTZ, BLYP/3-21G, and SCC-DFTB levels of theory in Fig. 6 and compare them to evaluate the accuracy of the SCC-DFTB DOS. These plots are obtained as a superposition of Gaussian peaks corresponding to discrete orbital energy levels. The Fermi level, determined as an averaged energy of the highest occupied MO (HOMO) and lowest unoccupied MO (LUMO) orbitals, is denoted with a vertical arrow labeled "FE" on each plot. Table V lists the Fermi levels for all three fullerenes at all three levels of theory; the differences between DFT and SCC-DFTB are on the order of 0.3 eV for C_{60} and C_{70} and much smaller for C_{28}, while the basis set effect is almost negligible. In case of C_{28}, FE is located at a maximum in DOS which coincides with the very small HOMO-LUMO gap in this molecule, whereas for the more stable C_{60} and C_{70} species, the FE is located at a minimum. For C_{28}, the FE is also lower at all levels of theory than C_{60} and C_{70}, indicating the strong electron deficiency of this unstable species. We also note that the Fermi level is located at almost the same energy of −4.7 eV in case of C_{60} and C_{70}, indicating similar redox properties for these species as has been demonstrated experimentally before.[56] Moreover, for each species, the DOS in the vicinity of the Fermi level and the DOS corresponding to occupied orbitals ("valence band") are very similar for all the methods and do not even differ much between individual fullerene species for the region down to −1.0 hartree; a large peak around −0.4 hartree is followed by two to three smaller peaks down to −0.8 hartree, after which the DOS rapidly drops to zero. The shape of the DOS corresponding to unoccupied orbitals ("conduction band") is strongly dependent on the size of basis set used for the calculations; generally speaking, the larger the basis set, the higher the DOS for unoccupied eigenstates. This trend can be clearly seen when a split valence double zeta (3-21G) basis set is compared with the highly polarized cc-pVTZ basis set at the BLYP level; features and absolute DOS are extremely different for both cases. Since SCC-DFTB uses a minimal valence basis set, its corresponding DOS in this region mimics more closely the BLYP/3-21G result. This rather intuitive finding suggests that SCC-DFTB can be potentially used for calculating only the lowest UV transitions within a time-dependent (TD) SCC-DFTB response analysis framework,[57] somewhat different to the situation of TD-DFT.[58]

IV. SUMMARY AND CONCLUSIONS

We have calculated optimized geometries, vibrational spectra, and vibrational and electronic density of states of three closed-shell fullerene D_2 C_{28}, I_h C_{60}, and D_{5h} C_{70} isomers using a variety of DFT and DFTB methods. The optimized geometries are reproduced with small deviations. SCC-DFTB and DFTB overestimate bond lengths by as much as 0.03 Å for all three fullerenes when compared with B3LYP/cc-pVTZ data, but only by 0.01 Å relative to BLYP/3-21G data. In a detailed analysis of unscaled harmonic vibrational frequencies, we find very interesting correlations between the root mean square deviations σ_{rms} of BLYP/6-31G(d), BLYP/3-21G, SCC-DFTB, and B3LYP/6-31G(d), with respect to the most accurate BLYP/cc-pVTZ level of theory and experiment; while C_{28} is somewhat special due to its high ring strain and low-lying virtual orbitals, the corresponding values of σ_{rms} are highly transferable between C_{60} and C_{70}, with approximately 18 cm^{-1} [BLYP/6-31G(d)], 40 cm^{-1} (BLYP/3-21G), 32 cm^{-1} (SCC-DFTB), and 45 cm^{-1} [B3LYP/6-31G(d)]. While it is true that B3LYP results can be systematically improved to match experiment better by applying a global scaling factor of about 0.98, the aim of our benchmark was to provide an "honest" comparison for each method itself and to see how SCC-DFTB performs with respect to its "originating" method, namely, generalized gradient approximation (GGA) DFT. In this sense, accuracy of the SCC-DFTB-predicted vibrational frequencies is of comparable or better quality than those from BLYP with small or medium basis sets. In the case of pentagon deformation modes around 600–700 cm^{-1}, we find that the basis set effect is very strong in this case and that BLYP/cc-pVTZ overshoots the experimental results somewhat, while SCC-DFTB and small basis set BLYP underestimate the frequencies of the same modes. Regarding the modeling of vibrational IR and Raman spectra of various fullerene structures, we find that the SCC-DFTB-predicted spectra show good correspondence to experiment and more elaborate theoretical findings. The quality of spectra is better for fullerenes with larger HOMO-LUMO gap. The SCC-DFTB vibrational density of states (VDOS) corresponds well to BLYP calculations and mimics small basis set results better. However, BLYP/cc-pVTZ VDOS features are generally reproduced rather well, although exact position and shape of SCC-DFTB VDOS features need to be treated with care. The SCC-DFTB electronic densities of states reproduce well the Fermi levels and densities of occupied and lowest virtual one-electron energy levels.

We conclude that the SCC-DFTB method can be safely employed for determination of vibrational properties of carbon fullerenes and nanotubes provided that the studied struc-

This article is copyrighted as indicated in the article. Reuse of AIP content is subject to the terms at: http://scitation.aip.org/termsconditions. Downloaded to IP: 140.113.38.11 On: Wed, 30 Apr 2014 06:23:16

tures have well-defined nonmetallic structure, i.e., the HOMO-LUMO gap is not too small. In this case, however, single-reference wave-function-based methods have to be employed with great care in general, and this restriction is not specific to the SCC-DFTB method itself.

ACKNOWLEDGMENTS

One of the authors (H.A.W.) would like to acknowledge the National Science Council of Taiwan for financial support (NCC95-2113-M-009-015). This work was partially supported by a grant from the Mitsubishi Chemical Corporation, and computer resources were provided in part by the Air Force Office of Scientific Research DURIP grant (FA9550-04-1-0321) and access to MSRC as well as by the Cherry L. Emerson Center of Emory University. The research was performed in part using the Molecular Science Computing Facility (MSCF) in the William R. Wiley Environmental Molecular Sciences Laboratory, a national scientific user facility sponsored by the U.S. Department of Energy's Office of Biological and Environmental Research and located at the Pacific Northwest National Laboratory, operated for the Department of Energy by Battettle. In supplemental materials, Table S1 lists Cartesian coordinates in angstroms of D_2 C_{28}, I_h C_{60}, and D_{5h} C_{70} isomers at the BLYP/cc-pVTZ, BLYP/6-31G(d), BLYP/3-21G, and SCC-DFTB levels of theory. Tables S2–S4 list computed BLYP/cc-pVTZ IR intensities and BLYP/6-31G(d), BLYP/3-21G, and SCC-DFTB IR intensities and Raman activities of D_2 C_{28}, I_h C_{60}, and D_{5h} C_{70}.

[1] E. Osawa, *Perspectives of Fullerene Nanotechnology*. Proceedings of the International Fullerenes Workshop, 2001 (Kluwer, Dordrecht, 2001); M. S. Dresselhaus, G. Dresselhaus, and P. Avouris, *Carbon Nanotubes: Synthesis, Structure, Properties, and Applications* (Springer, New York, 2001).
[2] G. Zheng, S. Irle, M. Elstner, and K. Morokuma, J. Phys. Chem. A **108**, 3182 (2004).
[3] S. Irle, G. Zheng, Z. Wang, and K. Morokuma, J. Phys. Chem. B **110**, 21135 (2006).
[4] T. P. Martin, U. Näher, H. Schaber, and U. Zimmermannn, Phys. Rev. Lett. **70**, 3079 (1993); A. Varykhalov, W. Gudat, V. K. Adamchuk, and O. Rader, Phys. Rev. B **73**, 241404(R) (2006).
[5] B. W. Smith, M. Monthioux, and D. E. Luzzi, Nature (London) **396**, 323 (1998); K. Hirahara, K. Suenaga, S. Bandow, H. Kato, T. Okazaki, H. Shinohara, and S. Iijima, Phys. Rev. Lett. **85**, 5384 (2000).
[6] M. Kallay and J. Gauss, J. Chem. Phys. **120**, 6841 (2004).
[7] J. Baker, K. Wolinski, M. Malagoli, and P. Pulay, Mol. Phys. **102**, 2475 (2004).
[8] S. Saebo and P. Pulay, Annu. Rev. Phys. Chem. **44**, 213 (1993).
[9] E. J. Baerends, D. E. Ellis, and P. Ros, Chem. Phys. **2**, 41 (1973); R. Polly, H.-J. Werner, F. R. Manby, and P. J. Knowles, Mol. Phys. **102**, 2311 (2004); S. Varga, M. Matus, and J. Noga, J. Chem. Phys. **124**, 034106 (2006); H.-J. Werner and F. R. Manby, *ibid.* **124**, 054114 (2006).
[10] O. Vahtras, J. Almlöf, and M. W. Feyereisen, Chem. Phys. Lett. **213**, 514 (1993); K. Eichkorn, O. Treutler, H. Öhm, M. Häser, and R. Ahlrichs, *ibid.* **240**, 283 (1995); P. Pulay, S. Saebo, and K. Wolinski, *ibid.* **344**, 543 (2001).
[11] W. Yang, Phys. Rev. Lett. **66**, 1438 (1991); Y. Shao, C. T. White, and M. Head-Gordon, J. Chem. Phys. **114**, 6572 (2001).
[12] J. C. Burant, M. C. Strain, G. E. Scuseria, and M. J. Frisch, Chem. Phys. Lett. **258**, 45 (1996); T. Hrenar, G. Rauhut, and H.-J. Werner, J. Phys. Chem. A **110**, 1089 (2006).
[13] D. Porezag, T. Frauenheim, T. Köhler, G. Seifert, and R. Kaschner, Phys. Rev. B **51**, 12947 (1995); T. Frauenheim, F. Weich, T. Köhler, S. Uhlmann, D. Porezag, and G. Seifert, *ibid.* **52**, 11492 (1995).
[14] M. Elstner, D. Porezag, G. Jungnickel, J. Elsner, M. Haugk, T. Frauenheim, S. Suhai, and G. Seifert, Phys. Rev. B **58**, 7260 (1998).
[15] M. J. S. Dewar, E. G. Zoebisch, E. F. Healy, and J. J. P. Stewart, J. Am. Chem. Soc. **107**, 3902 (1985).
[16] J. J. P. Stewart, J. Comput. Chem. **10**, 209 (1989).
[17] T. Frauenheim, G. Seifert, M. Elsterner, Z. Hajnal, G. Jungnickel, D. Porezag, S. Suhai, and R. Scholz, Phys. Status Solidi B **217**, 41 (2000).
[18] M. Elstner, Q. Cui, P. Munih, E. Kaxiras, T. Frauenheim, and M. Karplus, J. Comput. Chem. **24**, 565 (2003).
[19] G. Zheng, S. Irle, and K. Morokuma, Chem. Phys. Lett. **412**, 210 (2005).
[20] S. Irle, G. Zheng, M. Elstner, and K. Morokuma, Nano Lett. **3**, 1657 (2003); G. Zheng, S. Irle, and K. Morokuma, J. Chem. Phys. **122**, 014708 (2005); G. Zheng, Z. Wang, S. Irle, and K. Morokuma, J. Nanosci. Nanotechnol. (in press).
[21] H. Witek, S. Irle, and K. Morokuma, J. Chem. Phys. **121**, 5163 (2004).
[22] H. A. Witek, K. Morokuma, and A. Stradomska, J. Chem. Phys. **121**, 5171 (2004).
[23] H. A. Witek, K. Morokuma, and A. Stradomska, J. Theor. Comput. Chem. **4**, 639 (2005).
[24] E. Malolepsza, H. A. Witek, and K. Morokuma, Chem. Phys. Lett. **412**, 237 (2005).
[25] V. Schettino, M. Pagliai, L. Ciabini, and G. Cardini, J. Phys. Chem. A **105**, 11192 (2001).
[26] G. Sun and M. Kertesz, J. Phys. Chem. A **106**, 6381 (2002).
[27] J. S. Binkley, J. A. Pople, and W. J. Hehre, J. Am. Chem. Soc. **102**, 939 (1980).
[28] W. J. Hehre, R. Ditchfield, and J. A. Pople, J. Chem. Phys. **56**, 2257 (1972); P. C. Hariharan and J. A. Pople, Theor. Chim. Acta **28**, 213 (1973).
[29] T. H. Dunning, Jr., J. Chem. Phys. **90**(2), 1007 (1994).
[30] A. P. Scott and L. Radom, J. Phys. Chem. **100**, 16502 (1996).
[31] M. D. Halls, J. Velkovski, and H. B. Schlegel, Theor. Chem. Acc. **105**, 413 (2001).
[32] A. Becke, Phys. Rev. A **38**, 3098 (1988); C. Y. Lee, W. Yang, and R. G. Parr, Phys. Rev. B **37**, 785 (1988).
[33] A. D. Becke, J. Chem. Phys. **98**, 5648 (1993).
[34] M. J. Frisch, G. W. Trucks, H. B. Schlegel *et al.*, GAUSSIAN 03, Gaussian, Inc., Wallingford, CT, 2004.
[35] E. Aprà, T. L. Windus, T. P. Straatsma *et al.*, NWCHEM, a computational chemistry package for parallel computers, Version 4.7, Richland, WA, 2005.
[36] C. Kohler, G. Seifert, U. Gerstmann, M. Elstner, H. Overhof, and T. Frauenheim, Phys. Chem. Chem. Phys. **3**, 5109 (2001).
[37] H. Guo and M. Karplus, J. Chem. Phys. **94**(5), 3679 (1991).
[38] C. H. Choi, M. Kertesz, and A. Karpfen, J. Chem. Phys. **107**, 6712 (1997).
[39] C. H. Choi, M. Kertesz, and L. Mihaly, J. Phys. Chem. A **104**, 102 (2000).
[40] C. S. Yannoni, P. P. Bernier, D. S. Bethune, G. Meijer, and J. R. Salem, J. Am. Chem. Soc. **103**, 3192 (1991).
[41] K. Hedberg, L. Hedberg, D. S. Bethune, S. Donald, C. A. Borwn, H. C. Dorn, R. D. Johnson, and M. De Vries, Science **254**, 410 (1991).
[42] M. Ernzerhof and G. E. Scuseria, J. Chem. Phys. **110**, 5029 (1999).
[43] J. Neugebauer, M. Reiher, C. Kind, and B. A. Hess, J. Comput. Chem. **23**, 895 (2002).
[44] V. Schettino, M. Paglini, and G. Cardini, J. Phys. Chem. A **106**, 1815 (2002).
[45] D. S. Bethune, G. Meijer, W. C. Tang, H. J. Rosen, W. G. Golden, H. Seki, C. A. Brown, and M. S. de Vries, Chem. Phys. Lett. **179**, 181 (1991).
[46] R. E. Stratmann, G. E. Scuseria, and M. J. Frisch, J. Raman Spectrosc. **29**, 483 (1998).
[47] M. Kofranek, H. Lischka, and A. Karpfen, J. Chem. Phys. **96**, 982 (1992).
[48] P. Pulay, G. Fogarasi, F. Pang, and J. E. Boggs, J. Am. Chem. Soc. **101**, 2550 (1979).
[49] S. Irle and H. Lischka, J. Mol. Struct.: THEOCHEM **364**, 15 (1996).
[50] W. Brockner and F. Menzel, J. Mol. Struct. **378**, 147 (1996).
[51] F. Varga, L. Nemes, and J. K. G. Watson, J. Phys. B **29**, 5043 (1996).
[52] K. Lynch, C. Tanke, F. Menzel, W. Brockner, P. Scharff, and E. Stumpp, J. Phys. Chem. **99**, 7985 (1995).
[53] C. Z. Wang and K. M. Ho, Phys. Rev. Lett. **71**, 1184 (1993); H. Y. Zhang, X. Gu, X. H. Zhang, X. Ye, and X. G. Gong, Phys. Lett. A **331**, 332 (2004).

This article is copyrighted as indicated in the article. Reuse of AIP content is subject to the terms at: http://scitation.aip.org/termsconditions. Downloaded to IP: 140.113.38.11 On: Wed, 30 Apr 2014 06:23:16

[54] A. Hirsch, Z. Chen, and H. Jiao, Angew. Chem., Int. Ed. **39**, 3915 (2000).
[55] A. Yazdani and E. J. Mele, Appl. Phys. A: Mater. Sci. Process. **76**, 469 (2003); T. Okazaki and H. Shinohara, *Proceedings for Applied Physics of Carbon Nanotubes, 2005* (Springer, Berlin, 2005); S. Okada, S. Susumu, and O. Atsushi, Phys. Rev. Lett. **86**, 3835 (2001); O. Dubay and G. Kreese, Phys. Rev. B **70**, 165424 (2004).
[56] Q. Xie, E. Perez-Corderc, and L. Echegoyen, J. Am. Chem. Soc. **114**, 3978 (1992); F. Zhou, C. Jeboulet, and A. J. Bard, *ibid.* **114**, 11004 (1992); R. Volpel, G. Hofmann, M. Steidl, M. Stenke, M. Schlapp, R. Trassl, and E. Salzborn, Phys. Rev. Lett. **71**, 3439 (1993).
[57] T. A. Niehaus, S. Suhai, F. Della Sala, P. Lugli, M. Elstner, G. Seifert, and T. Frauenheim, Phys. Rev. B **63**, 085108 (2001).
[58] R. Bauernschmitt and R. Ahlrichs, Chem. Phys. Lett. **256**, 454 (1996).
[59] See EPAPS Document No. E-JCPSA6-125-705642 for supplemental material. This document can be reached via a direct link in the online article's HTML reference section or via the EPAPS homepage (http://www.aip.org/pubservs/epaps.html).

This article is copyrighted as indicated in the article. Reuse of AIP content is subject to the terms at: http://scitation.aip.org/termsconditions. Downloaded to IP: 140.113.38.11 On: Wed, 30 Apr 2014 06:23:16